High resolution simulations of a tornadic storm affecting Sydney

J. Hartigan[1] S. MacNamara[2] L. M. Leslie[3]
M. S. Speer[4]

(Received 28 December 2020; revised 6 May 2021)

Abstract

On 16 December 2015 a severe thunderstorm and associated tornado affected Sydney causing widespread damage and insured losses of $206 million. Severe impacts occurred in Kurnell, requiring repairs to Sydney's desalination plant which supplies up to 15% of Sydney water during drought, with repairs only completed at the end of 2018. Climatologically, this storm was unusual as it occurred during the morning and had developed over the ocean, rather than developing inland during the afternoon as is the case for many severe storms impacting the Sydney region. Simulations of the Kurnell storm were conducted using the Weather Research and Forecasting (WRF) model on a double nested domain using the Morrison microphysics scheme and the NSSL 2-moment 4-ice microphysics scheme. Both simulations produced severe

DOI:10.21914/anziamj.v62i0.16113, Published 2021-05-23, as part of the Proceedings of the 19th Biennial Computational Techniques and Applications Conference. ISSN 1445-8810. (Print two pages per sheet of paper.)

storms that followed paths similar to the observed storm. However, the storm produced under the Morrison scheme did not have the same morphology as the observed storm. Meanwhile, the storm simulated with the NSSL scheme displayed cyclical low- and mid-level mesocyclone development, which was observed in the Kurnell storm, highlighting that the atmosphere supported the development of severe rotating thunderstorms with the potential for tornadogenesis. The NSSL storm also produced severe hail and surface winds, similar to observations. The ability of WRF to simulate general convective characteristics and a storm similar to that observed displays the applicability of this model to study the causes of severe high-impact Australian thunderstorms.

Contents

1 Introduction

At approximately 10:30 AM local time (UTC+11 hours), on 16 December 2015, an EF2 rated tornado [13] impacted the Sydney suburb of Kurnell. The storm and associated tornado was the most costly natural disaster of the Australian 2015/2016 summer, with insured losses of AU$206 million [5]. The Sydney desalination plant was heavily impacted and required major repairs that were not completed until the end of 2018, months before needing to be used during the intense drought in 2019. Furthermore, the tornado was located only 4 km

southeast of Sydney airport, Australia's busiest airport.

The storm itself was unusual as it developed during the morning and over the ocean, rather than the usual development inland during the afternoon, associated with maximum daytime heating and Convective Available Potential Energy (CAPE); this afternoon or evening storm development is more typical of severe thunderstorms in the Sydney region [1, 14]. Additionally, observational evidence suggests that this storm potentially produced multiple tornadoes over its lifetime [11].

Numerical simulations of severe convective storms can provide detailed information not available from routine weather observations. The output from these simulations can be used to better understand how storms developed and intensified, and how specific storm-related hazards were supported by the atmosphere. In this study, high resolution simulations are performed using the Weather Research and Forecasting (WRF) model [10] as an initial investigation into the characteristics of the storm.

2 Data and methodology

The WRF model was configured on a double-nested domain centred on Sydney. The outer nest is $1050 \times 1050\,\mathrm{km}^2$ with $1.5\,\mathrm{km}$ horizontal resolution, while the inner nest is $450.5 \times 500\,\mathrm{km}^2$ with $0.5\,\mathrm{km}$ resolution. The model top is set at $50\,\mathrm{hPa}$, with 33 vertical levels stretching from a resolution of approximately $52\,\mathrm{m}$ at the model surface to $1093\,\mathrm{m}$ at the model top. The governing equations of the model are the non-hydrostatic Euler equations:

$$\partial_t U + \nabla \cdot \mathbf{V} u + \mu_d \alpha \partial_x p + (\alpha/\alpha_d)\, \partial_\eta p \partial_x \phi = F_U\,, \tag{1}$$

$$\partial_t V + \nabla \cdot \mathbf{V} v + \mu_d \alpha \partial_y p + (\alpha/\alpha_d)\, \partial_\eta p \partial_y \phi = F_V\,, \tag{2}$$

$$\partial_t W + \nabla \cdot \mathbf{V} w - g\,[(\alpha/\alpha_d)\, \partial_\eta p - \mu_d] = F_W\,, \tag{3}$$

$$\partial_t \Theta_m + \nabla \cdot \mathbf{V} \theta_m = F_{\Theta_m} \tag{4}$$

$$\partial_t \mu_d + \nabla \cdot \mathbf{V} = 0\,, \tag{5}$$

$$\partial_t \phi + \mu_d^{-1}\,[(\mathbf{V} \cdot \nabla \phi) - g W] = 0\,, \tag{6}$$

$$\partial_t Q_m + \nabla \cdot \mathbf{V} q_m = F_{Q_m}\,, \tag{7}$$

where $\boldsymbol{\nu} = (u, v, w)$ represents the zonal, meridional and vertical components of wind, θ_m is moist potential temperature, $\phi = gz$ is the geopotential with height z, g is gravitational acceleration, p is the full pressure, q_m represents moisture mixing ratios, μ_d is the vertical coordinate metric, α_d is the inverse density of dry air, α is the inverse density of the full parcel and η is a terrain-following hydrostatic pressure vertical coordinate. Furthermore, $\mathbf{V} = \mu_d \boldsymbol{\nu} = (U, V, W)$, $\Theta_m = \mu_d \theta_m$ and $Q_m = \mu_d q_m$. The right hand sides of the governing equations represent forcing terms from model physics, turbulent mixing, spherical projections and Earth's rotation. Finally, the diagnostic equation for hydrostatic pressure is

$$\partial_\eta \phi = -\alpha_d \mu_d\,. \tag{8}$$

The model is solved with an integration time step of 3 s, using a time-splitting third-order Runge–Kutta scheme, where acoustic modes are integrated over a shorter time step. For more details on the model equations, and how they are solved, the reader is referred to the WRF technical notes [12].

Microphysical parameterisation describes various cloud-scale processes such as evaporation and melting. These processes can be represented differently, affecting the resulting storm morphology [3]. As such, this study has performed simulations using the Morrison [8, 9] and the NSSL 2-moment 4-ice [6] microphysics schemes, which are represented in the same way on both domains. The Morrison scheme predicts the mass of cloud, rain, ice, snow, and hail, and the number concentration of all these particles except cloud drops. Whereas the NSSL scheme predicts the mass and number concentration of cloud, rain, ice, snow, graupel, and hail. These schemes utilise different equations to describe the mass, number concentration and terminal fall velocity of particles which could significantly affect the simulation results. In order to simplify the results, the simulations presented here did not include longwave or shortwave radiation, boundary layer physics or surface physics.

The initial and boundary conditions used in this study are the European Centre for Medium-Range Weather Forecast's (ECMWF) ERA5 reanalysis data

set [4], which was originally on a 30 km grid, and has been interpolated to the 1.5 km outer domain. The simulations are set to begin on 15/12/2015 at 0000 UTC, and end on 16/12/2015 at 0900 UTC. The inner domain data was output every 5 min, while the outer domain was output every 15 min.

3 Event overview

Over the course of the morning, a high pressure system was located off the southeast coast of Australia, directing moist surface easterly winds over New South Wales (NSW; Figure 1(a)). Meanwhile, a 500 hPa trough and associated cold pool extended from the southeast coast inland towards the northwest of the continent (Figure 1(b)). This resulted in a broad region of unstable air along the NSW coast, with highly unstable air concentrated over the Sydney region and adjacent ocean (CAPE $\geqslant 1000\,\mathrm{J\,kg^{-1}}$, TT $\geqslant 50\,\mathrm{K}$; Figure 1(c,d)). The marine boundary layer was capped in the early morning; however, this cap was removed during the morning likely due to moistening and cooling of the atmosphere above the marine boundary layer [11].

Prior to development of the Kurnell tornadic storm, there was some weak convection over the Great Dividing Range extending into the Sydney and central coast regions (not shown). A cluster of convection developed off the Illawarra coast at approximately 1700 UTC 2015-12-15 (not shown). The Kurnell tornadic storm developed from the merging of two cells near Kiama at 2100 UTC (not shown). The storm tracked north, adjacent to the coast, as a supercell thunderstorm. It then crossed the coastline and tracked through Kurnell, producing an EF2 rated tornado (Figure 2). After passing through Kurnell and the eastern suburbs of Sydney, the storm moved offshore in a northeasterly direction and dissipated.

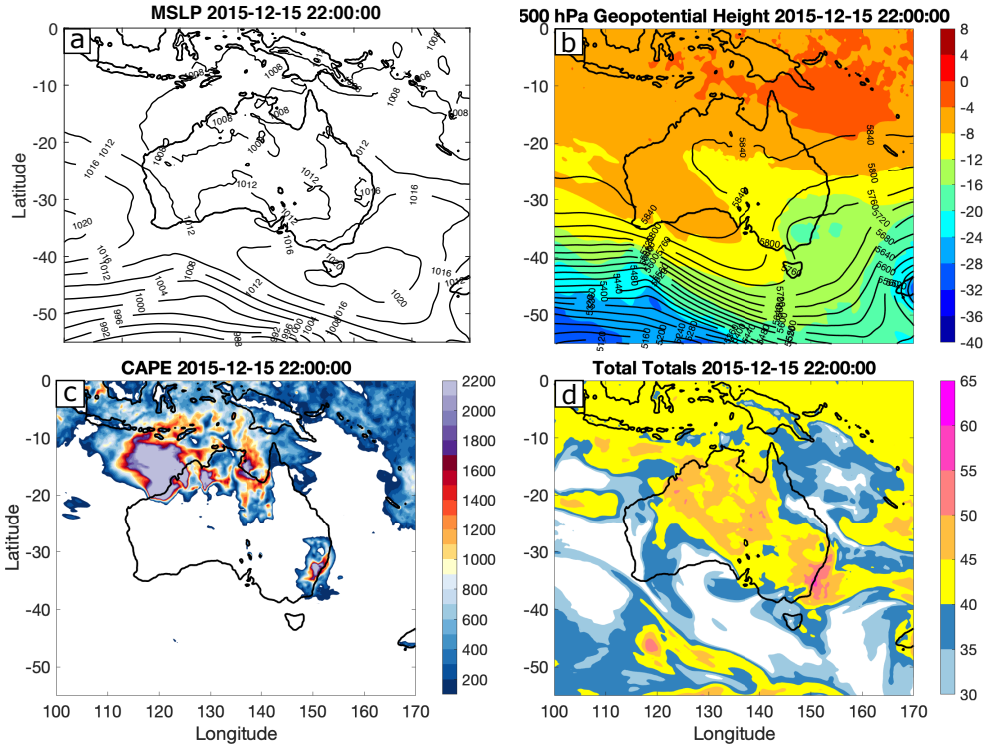

Figure 1: Atmospheric conditions from ERA5 reanalysis data, at the time of development of the Kurnell tornadic storm. Variables shown are (a) mean sea level pressure (hPa); (b) 500 hPa geopotential height (m) represented as thin black contours, and temperature (°C) represented by filled contours; (c) convective available potential energy (CAPE; $J\,kg^{-1}$); and (d) total totals index (TT; K [7]).

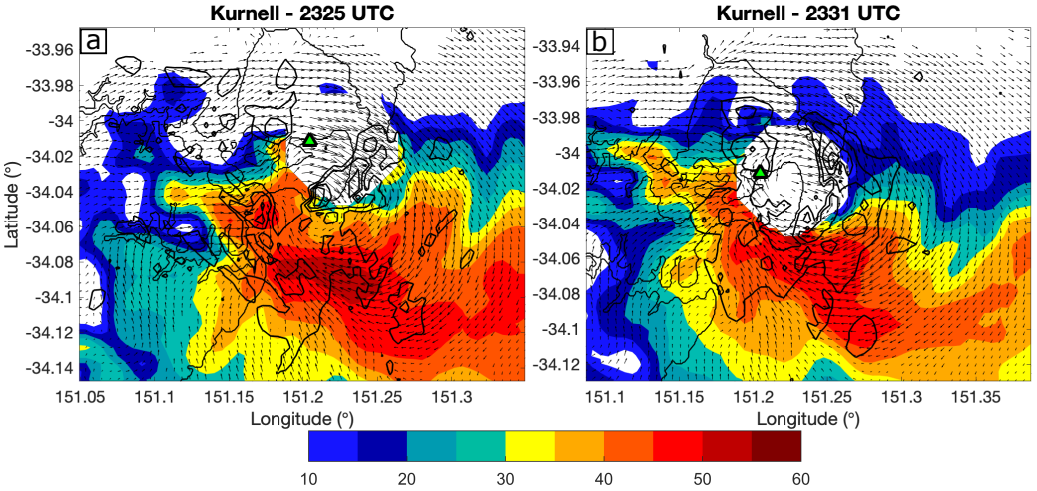

Figure 2: Filled contours display radar reflectivity (dBZ), thin black contours are vertical velocity (every $10\,\mathrm{m\,s^{-1}}$ starting at $5\,\mathrm{m\,s^{-1}}$), and vectors show wind speed and direction, from the Kurnell radar interpolated to 2.5 km above sea level, at (a) 2325 UTC and (b) 2331 UTC. The location of Kurnell is provided by a solid green triangle. White regions are where no reflectivity is observed by the radar. The white circle in the figure is due to the storm propagating over the Kurnell radar, where sampling does not take place. However, vectors still exist in this circle as the 3D wind field is retrieved using multiple radars that sample this region.

4 Simulation results

Similar to observations, both simulations display convection forming off the Illawarra coast at 1600 UTC, with additional weak convection occurring inland of the Sydney and central coast region (not shown). Both microphysics schemes display a merging of two cells near Kiama, resulting in one strong storm cell propagating over the ocean adjacent to the coast, although this occurs approximately one hour earlier than the observed cell. Additionally, the storm produced in the Morrison scheme displays a quasi-linear convective

system (QLCS) morphology, rather than supercell morphology (not shown). The Morrison scheme produces a larger and stronger cold pool (not shown). Investigation into the causes of this is beyond the scope of the present article but could be due to greater numbers of small rain particles being simulated in the Morrison scheme, leading to greater evaporative cooling, or it could be due to smaller hail being simulated, leading to greater cooling through melting. This larger and stronger cold pool in the Morrison scheme could lead to environmental interactions that favour a QLCS mode. Due to the difference in the simulated convective mode under the Morrison scheme, the results herein will focus on the simulation that used NSSL microphysics.

The NSSL storm enters the inner domain at approximately 2115 UTC, with one main updraft that is located immediately behind the leading edge of the cold pool (not shown). This storm begins displaying mid-level updraft rotation at 2150 UTC (not shown), followed by the development of a hook echo at the lowest model level at 2215 UTC (Figure 3(a)), which is a common radar characteristic of supercell convection, and an area where tornadogenesis is most likely to occur. Additionally, there is a clearly defined rear flank gust front intersecting with the forward flank gust front at the hook echo region, with strong inflow directed into this area (Figure 3). This low-level mesocyclone initially draws in warmer environmental air from ahead of the gust front (Figure 4(a)). However, strong outflow on the rear flank appears to push the rear flank gust front away from the low-level mesocyclone (Figure 4(b)). This likely caused the demise of the first vortex at 2330 UTC, due to ingestion of cooler, more stable air.

The simulated storm is in the vicinity of Kurnell at 2240 UTC (Figure 3(b)), and continues propagating north through Sydney. Another low-level mesocyclone develops over the ocean at 2240 UTC, becoming clearly defined at 2245 UTC (Figures 3(b) and 4(c)). This mesocyclone progresses along the rear flank gust front towards the forward flank gust front, dragging warm inflow air into its circulation at 2300 UTC before dissipating (Figure 4(d)). It is possible that interactions of the low-level mesocyclone with the forward flank gust front led to its demise. After the storm passes through Sydney, it begins

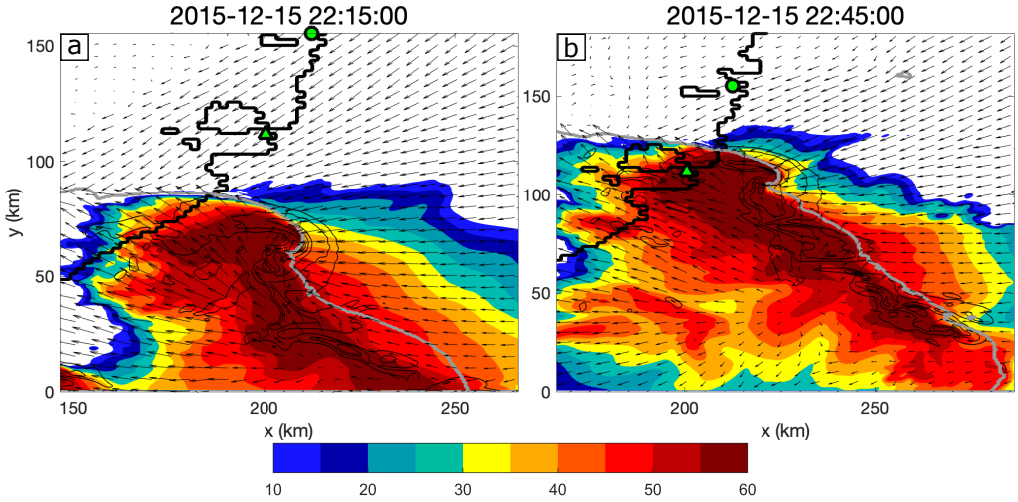

Figure 3: Variables shown are lowest model level reflectivity (filled contours; dBZ), wind speed and direction (vectors), and cold pool outline (thick grey contour representing $\theta' < -1\,\mathrm{K}$), and mid-level vertical velocity (eta-level = 17 approximately 5 km above sea level, thin black contours; every $10\,\mathrm{m\,s^{-1}}$ beginning at $5\,\mathrm{m\,s^{-1}}$), for the NSSL simulation. The location of Sydney is provided by a solid green circle, and the location of Kurnell is provided by a solid green triangle.

to propagate towards the east-northeast and change morphology into a QLCS. The storm is supported by convergence with the cold pool boundary against the northeasterly flow in the marine layer for some time until dissipating (not shown).

During the course of the event, there were numerous reports of wind gusts over $100\,\mathrm{km\,h^{-1}}$ and hail at most 6 cm in diameter across Sydney [2]. Figure 5 displays swath plots of maximum wind speed at 10 m, and maximum hail diameter at the surface, between 2210 and 2320 UTC from the NSSL simulation. The surface wind swath displays a large region of wind speeds over $25\,\mathrm{m\,s^{-1}}$, with some areas above $30\,\mathrm{m\,s^{-1}}$ (Figure 5(b)). Furthermore, the maximum

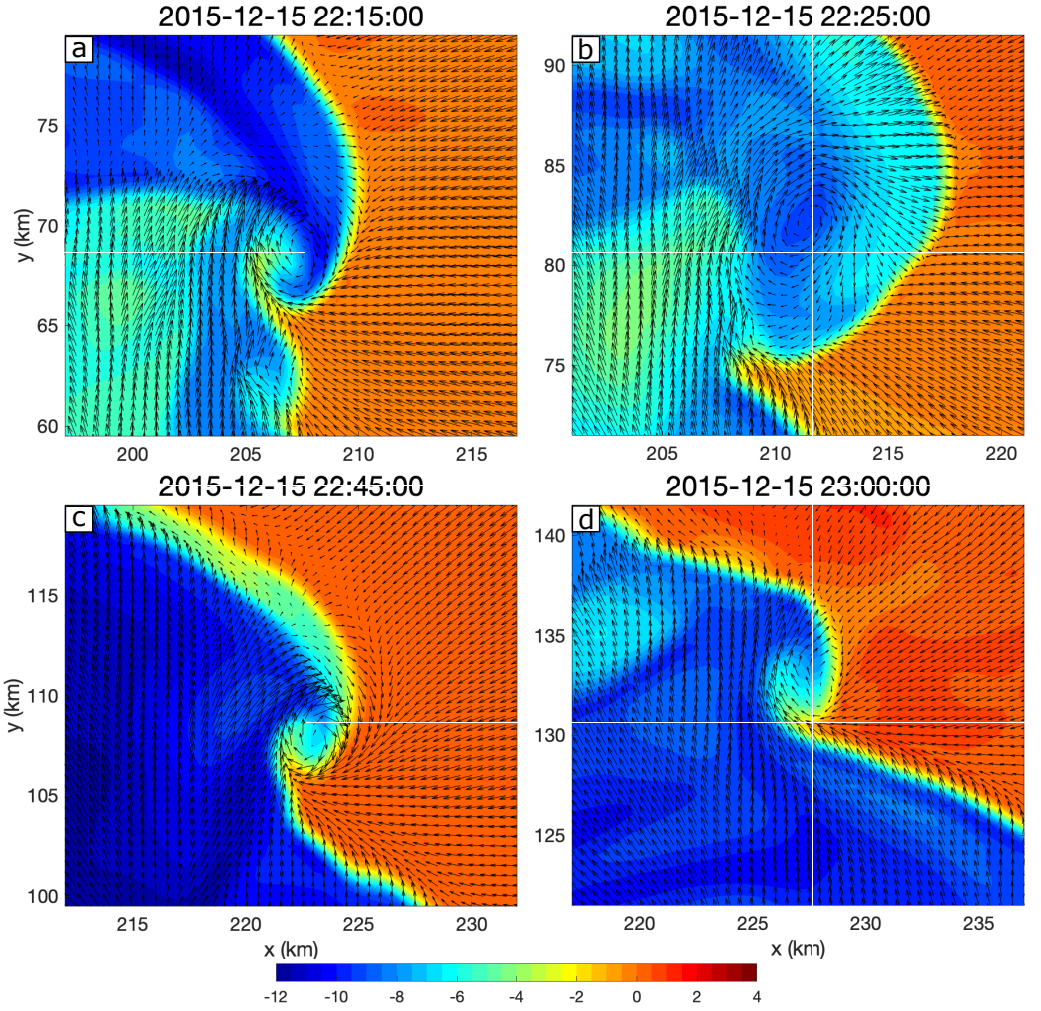

Figure 4: Filled contours display moist potential temperature perturbations (K) at the lowest model level, while vectors display lowest model level wind speed ($\mathrm{m\,s^{-1}}$) and direction. All figures are from the NSSL simulation. This figure is focused on the region of rotation, so the coastline is not included but is immediately to the left of the domain shown.

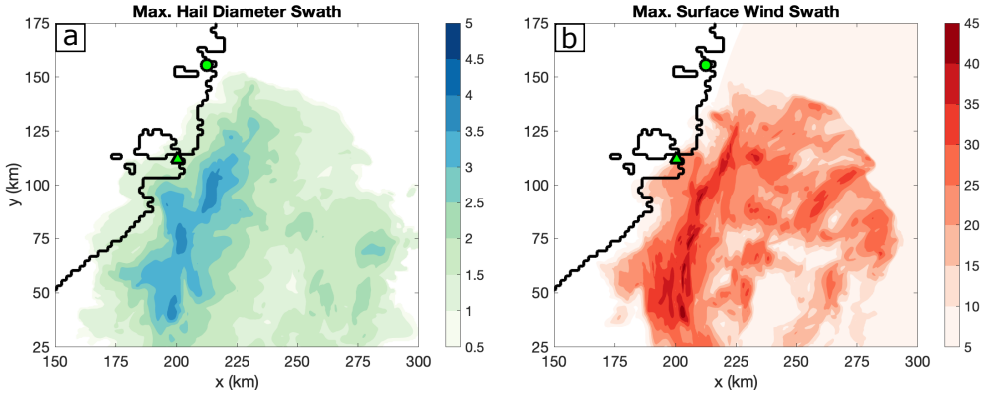

Figure 5: Simulated (a) maximum surface hail diameter (cm) and (b) maximum 10 m wind speed ($m\,s^{-1}$), between 2210 and 2320 UTC for the NSSL simulation. The location of Sydney is provided by a solid green circle, and the location of Kurnell is provided by a solid green triangle.

hail diameter swath indicates a relatively narrow region of hail between 3 and 4 cm in diameter (Figure 5(b)). Although the severe surface winds and hail all occur offshore in this simulated storm, rather than in parts of Sydney, the simulation indicates the environment was supportive of storms that could produce numerous severe weather hazards.

5 Conclusions and future work

In this study, two simulations of the tornadic storm that impacted Kurnell, Sydney, were performed using the WRF model with initial and boundary conditions from the ECMWF's ERA5 reanalysis data set. Although the simulations did not include longwave or shortwave radiation, boundary layer or surface physics, they both accurately depict the development of a storm at a similar time and location, and through similar mechanisms as the observed Kurnell storm.

Additionally, both simulations display this storm propagating north along the coast before impacting the Kurnell and Sydney region, and propagating back out to sea where it dissipates. This is despite the storm simulated under the Morrison microphysics scheme displaying a different morphology to that of the Kurnell and NSSL storms. Storm trajectories typically are dependent on the storm morphology due to the way the storm interacts with the ambient environment and maintains its structure. The tendency for both simulated storms to follow similar development patterns and trajectories, despite different microphysics schemes, was very promising. This similarity in the simulations indicates how strongly supportive the environment was for a severe convection event to develop near Sydney. However, the different storm morphology simulated in the Morrison microphysics scheme also highlights the importance of the common practice of running simulations using more than one microphysical scheme, in both research and operational settings, to capture a range of possible storm morphologies.

The storm simulated under the NSSL scheme displayed supercell characteristics, with both mid-level and low-level rotation evident. This rotation was cyclical, which was observed by Doppler radar on the day [11], providing further evidence that the storm could have produced numerous tornadoes over the ocean prior to impacting Kurnell. The NSSL storm also produced large hail and severe surface winds, although they were simulated over the ocean rather than in the Kurnell and greater Sydney region as observed. This difference is possibly due to the exclusion of surface and boundary layer physics in the model, although the results presented here are still remarkably accurate. Future work will focus on producing higher resolution simulations using the entire model physics. This will allow detailed vorticity and parcel trajectory analysis in order to better understand the contributing factors to tornadogenesis. Additionally, the Bureau of Meteorology's BARRA reanalysis data set, which is higher resolution than ERA5, will be used for initial and boundary conditions in future simulations. The results will be compared against those from ERA5, as the higher resolution would allow for higher resolution simulations to be performed at a lower computational cost.

Acknowledgements Alain Protat (Bureau of Meteorology) is thanked for the provision of radar observations and retrieved vertical velocity data of the Kurnell storm. We thank two anonymous reviewers for their suggestions which have improved the quality of the manuscript.

References

[1] J. T. Allen and E. R. Allen. "A review of severe thunderstorms in Australia". In: *Atmos. Res.* 178 (2016), pp. 347–366. DOI: 10.1016/j.atmosres.2016.03.011 (cit. on p. C3).

[2] Bureau of Meteorology. *Severe Storms Archive*. 2020. URL: http://www.bom.gov.au/australia/stormarchive/ (cit. on p. C9).

[3] D. T. Dawson II, M. Xue, J. A. Milbrandt, and M. K. Yau. "Comparison of evaporation and cold pool development between single-moment and multimoment bulk microphysics schemes in idealized simulations of tornadic thunderstorms". In: *Month. Wea. Rev.* 138 (2010), pp. 1152–1171. DOI: 10.1175/2009MWR2956.1 (cit. on p. C4).

[4] H. Hersbach, B. Bell, P. Berrisford, S. Hirahara, A. Horányi, J. Muñoz-Sabater, J. Nicolas, C. Peubey, R. Radu, D. Schepers, et al. "The ERA5 global reanalysis". In: *Quart. J. Roy. Meteor. Soc.* 146 (2020), pp. 1999–2049. DOI: 10.1002/qj.3803 (cit. on p. C5).

[5] Insurance Council of Australia. *Victorian bushfire losses push summer catastrophe bill past $550m*. 2016 (cit. on p. C2).

[6] E. R. Mansell, C. L. Ziegler, and E. C. Bruning. "Simulated electrification of a small thunderstorm with two-moment bulk microphysics". In: *J. Atmos. Sci.* 67 (2010), pp. 171–194. DOI: 10.1175/2009JAS2965.1 (cit. on p. C4).

[7] R. C. Miller. *Notes on analysis and severe-storm forecasting procedures of the Air Force Global Weather Central*. Vol. 200. Air Weather Service, 1972, 190 pp. URL: https://apps.dtic.mil/sti/citations/AD0744042 (cit. on p. C6).

[8] H. Morrison, J. A. Curry, and V. I. Khvorostyanov. "A new double-moment microphysics parameterization for application in cloud and climate models. Part I: Description". In: *J. Atmos. Sci.* 62 (2005), pp. 1665–1677. DOI: 10.1175/JAS3446.1 (cit. on p. C4).

[9] H. Morrison, G. Thompson, and V. Tatarskii. "Impact of cloud microphysics on the development of trailing stratiform precipitation in a simulated squall line: Comparison of one- and two-moment schemes". In: *Month. Wea. Rev.* 137 (2009), pp. 991–1007. DOI: 10.1175/2008MWR2556.1 (cit. on p. C4).

[10] J. G. Powers, J. B. Klemp, W. C. Skamarock, C. A. Davis, J. Dudhia, D. O. Gill, J. L. Coen, D. J. Gochis, R. Ahmadov, S. E. Peckham, et al. "The Weather Research and Forecasting Model: Overview, system efforts, and future directions". In: *Bull. Am. Meteor. Soc.* 98 (2017), pp. 1717–1737. DOI: 10.1175/BAMS-D-15-00308.1 (cit. on p. C3).

[11] H. Richter, A. Protat, J. Taylor, and J. Soderholm. "Doppler radar and storm environment observations of a maritime tornadic supercell in Sydney, Australia". In: *Preprints, 28th Conf. on Severe Local Storms, Portland OR, Amer. Meteor. Soc. P.* 2016 (cit. on pp. C3, C5, C12).

[12] W. C. Skamarock, J. B. Klemp, J. Dudhia, D. O. Gill, Z. Liu, J. Berner, W. Wang, J. G. Powers, M. G. Duda, D. Barker, and X.-Y. Huang. *A description of the advanced research WRF Model version 4*. Tech. rep. National Center for Atmospheric Research, Boulder CO, USA, 2019, p. 162. DOI: 10.5065/1dfh-6p97 (cit. on p. C4).

[13] Storm Prediction Center. *The Enhanced Fujita Scale (EF Scale)*. 2014. URL: https://www.spc.noaa.gov/efscale/ (cit. on p. C2).

[14] R. A. Warren, H. A. Ramsay, S. T. Siems, M. J. Manton, J. R. Peter, A. Protat, and A. Pillalamarri. "Radar-based climatology of damaging hailstorms in Brisbane and Sydney, Australia". In: *Quart. J. Roy. Meteor. Soc.* 146 (2020), pp. 505–530. DOI: 10.1002/qj.3693 (cit. on p. C3).

Author addresses

1. **J. Hartigan**, School of Mathematical and Physical Sciences, University of Technology Sydney, Ultimo, New South Wales 2007, Australia.
mailto:Joshua.Hartigan@student.uts.edu.au
orcid:0000-0002-7783-9440

2. **S. MacNamara**, ARC Centre of Excellence for Mathematical and Statistical Frontiers, School of Mathematical and Physical Sciences, University of Technology Sydney, Ultimo, New South Wales 2007, Australia.

3. **L. M. Leslie**, School of Mathematical and Physical Sciences, University of Technology Sydney, Ultimo, New South Wales 2007, Australia.
orcid:0000-0001-5616-2330

4. **M. S. Speer**, School of Mathematical and Physical Sciences, University of Technology Sydney, Ultimo, New South Wales 2007, Australia.
orcid:0000-0003-0421-7744